

## Design of electron wave filters in monolayer graphene by tunable transmission gap

Xi Chen and Jia-Wei Tao

Citation: *Applied Physics Letters* **94**, 262102 (2009); doi: 10.1063/1.3168527

View online: <http://dx.doi.org/10.1063/1.3168527>

View Table of Contents: <http://scitation.aip.org/content/aip/journal/apl/94/26?ver=pdfcov>

Published by the AIP Publishing

---

### Articles you may be interested in

[Photon induced tunneling of electron through a graphene electrostatic barrier](#)

*J. Appl. Phys.* **114**, 183706 (2013); 10.1063/1.4829446

[Transmission of electron through monolayer graphene laser barrier](#)

*Appl. Phys. Lett.* **100**, 183107 (2012); 10.1063/1.4710525

[A tunable electron wave filter based on graphene superlattices with periodic potential patterns](#)

*Appl. Phys. Lett.* **99**, 072108 (2011); 10.1063/1.3626278

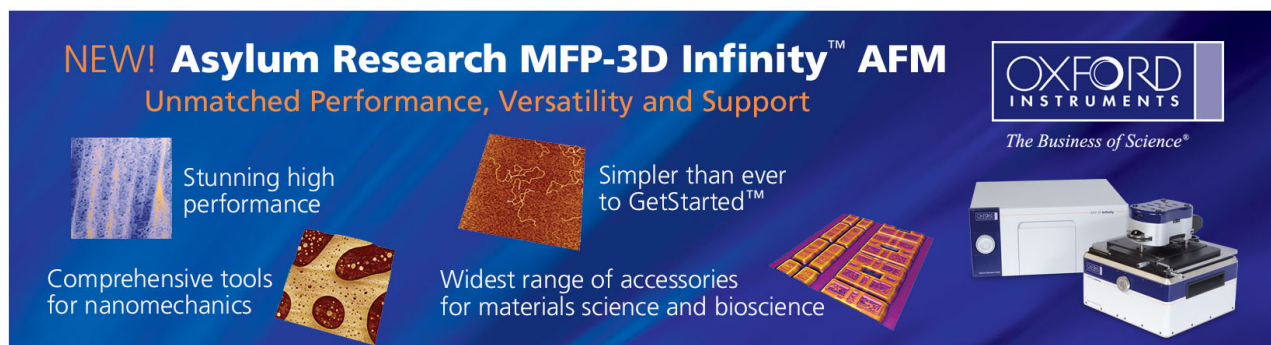
[Signature of quantum interference and the Fano resonances in the transmission spectrum of bilayer graphene nanostructure](#)

*J. Appl. Phys.* **110**, 014306 (2011); 10.1063/1.3603005

[Graphene on gold: Electron density of states studies by scanning tunneling spectroscopy](#)

*Appl. Phys. Lett.* **95**, 113114 (2009); 10.1063/1.3231440

---

This is a promotional banner for the Oxford Instruments Asylum Research MFP-3D Infinity AFM. The background is a deep blue gradient. On the left, the text 'NEW! Asylum Research MFP-3D Infinity™ AFM' is written in white and orange, followed by 'Unmatched Performance, Versatility and Support' in orange. Below this, there are four distinct sections, each with a small image and a text description: 1) 'Stunning high performance' with a blue and white image of a surface scan; 2) 'Simpler than ever to GetStarted™' with a brown and orange image of a surface scan; 3) 'Comprehensive tools for nanomechanics' with a yellow and brown image of a surface scan; 4) 'Widest range of accessories for materials science and bioscience' with a yellow and brown image of a surface scan. On the right side of the banner, the Oxford Instruments logo is displayed, consisting of the word 'OXFORD' above 'INSTRUMENTS' in a white box, with the tagline 'The Business of Science®' below it. At the bottom right, there is a photograph of the MFP-3D Infinity AFM system, which includes a large white base unit and a smaller, more complex scanning head unit.

# Design of electron wave filters in monolayer graphene by tunable transmission gap

Xi Chen<sup>1,2,a)</sup> and Jia-Wei Tao<sup>1</sup>

<sup>1</sup>Department of Physics, Shanghai University, 200444 Shanghai, People's Republic of China

<sup>2</sup>Departamento de Química-Física, UPV-EHU, Apdo 644, 48080 Bilbao, Spain

(Received 14 May 2009; accepted 11 June 2009; published online 29 June 2009)

We have investigated the transmission in monolayer graphene barrier at nonzero angle of incidence. Taking the influence of parallel wave vector into account, the transmission as the function of incidence energy has a gap due to the evanescent waves in two cases of Klein tunneling and classical motion. The modulation of the transmission gap by the incidence angle, the height, and width of potential barrier may lead to potential applications in graphene-based electronic devices. © 2009 American Institute of Physics. [DOI: 10.1063/1.3168527]

Graphene has become a subject of intense interest<sup>1,2</sup> since the graphitic sheet of one-atom thickness has been experimentally realized by Novoselov *et al.*<sup>3</sup> in 2004. The valence electron dynamics in such a truly two-dimensional (2D) material is governed by a massless Dirac equation. As a result, graphene exhibits many unique electronic and transport properties<sup>4,5</sup> such as the half-integer quantum Hall effect<sup>6–8</sup> and minimum conductivity.<sup>6</sup> Furthermore, another one is the perfect transmission, in particular, for normal incidence, through arbitrarily high and wide graphene barriers, which is referred to as Klein tunneling.<sup>9</sup> All these properties are significant in the design of various graphene-based devices, and graphene is thus regarded as a perspective base for the postsilicon electronics.

Until recently, the transport properties of massless Dirac fermions, including Klein tunneling and resonance transmission, have been extensively studied in the single or double graphene barriers and graphene superlattices.<sup>9–12</sup> However, inhomogeneous magnetic fields on the nanometer scale has been lately suggested to circumvent Klein tunneling and produce confined graphene-based structures.<sup>13–15</sup> It was found that the angular range of the transmission through monolayer or bilayer graphene with magnetic barrier structures could be efficiently controlled and resulted in the direction-dependent wave vector filter.<sup>16,17</sup>

In this letter, we will investigate the transmission of Dirac-like electrons in 2D monolayer graphene barrier at nonzero incidence angle. It is shown that when the electrons are obliquely incident on the potential barrier, the transmission has a gap, which depends strongly on the incidence angle, the width, and height of the barrier. This tunable transmission gap is quite different from the perfect transparency for the normal incidence<sup>9</sup> and does result from evanescent waves in two cases of Klein tunneling and classical motion due to the influence of parallel wave vector. In fact, based on the mechanism of Klein tunneling, a single graphene barrier is equivalent to a more complicated resonant tunneling device in common semiconductor heterostructures, at least from the point of view of the transmission.<sup>18</sup> Thus, these phenomena will provide a completely different mechanism of electron wave filters at the nanoscale level with more flex-

ibility and simplicity in design than those in multiple semiconductor quantum wells.<sup>19</sup>

Consider the ballistic electrons with Fermi energy  $E$  at angle  $\phi$  with respect to the  $x$  axis incident upon a 2D potential barrier, as shown in Fig. 1, where the tunable potential barrier is formed by a bipolar junction ( $p$ - $n$ - $p$ ) within a single-layer graphene sheet with top gate voltage  $V_g$ ,<sup>20</sup>  $V_0$  and  $d$  are the height and width of potential barrier, respectively. Since graphene is a 2D zero-gap semiconductor with the linear dispersion relation  $E = \hbar k_F v_F$ , the electrons are formally described by the Dirac-like Hamiltonian<sup>9</sup>  $\hat{H}_0 = -i\hbar v_F \sigma \nabla$ , where  $v_F \approx 10^6$  m s<sup>-1</sup> is the Fermi velocity,  $k_F$  is the Fermi wave vector, and  $\sigma = (\sigma_x, \sigma_y)$  are the Pauli matrices. The wave function of the incident electrons is assumed to be

$$\Psi_{in}(x, y) = \begin{pmatrix} 1 \\ s e^{i\phi} \end{pmatrix} e^{i(k_x x + k_y y)}. \quad (1)$$

The wave function of the transmitted one can be thus expressed by

$$\Psi_t(x, y) = t \begin{pmatrix} 1 \\ s e^{i\phi} \end{pmatrix} e^{i(k_x x + k_y y)}, \quad (2)$$

where  $k_x = k_F \cos \phi$  and  $k_y = k_F \sin \phi$  are the perpendicular and parallel wave vector components outside the barrier,  $k'_F = |E - V_0| / \hbar v_F$ ,  $q_x = (k'^2_F - k_y^2)^{1/2}$ ,  $\theta = \arctan(k_y / q_x)$ ,  $s = \text{sgn}(E)$ , and  $s' = \text{sgn}(E - V_0)$ . According to the boundary conditions, the transmission coefficient is determined by

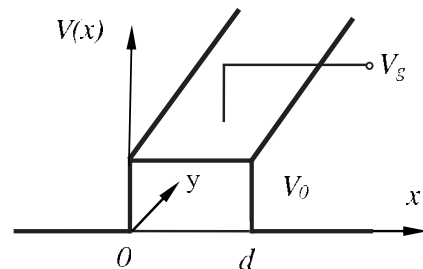


FIG. 1. Schematic diagram for 2D graphene barrier.

<sup>a)</sup>Electronic mail: xchen@shu.edu.cn.

$$t = \frac{2ss' \cos \phi \cos \theta}{ss' [e^{-iq_x d} \cos(\phi + \theta) + e^{iq_x d} \cos(\phi - \theta)] - 2i \sin(q_x d)}. \quad (3)$$

In what follows, we will discuss the transmission and reflection in two different cases of Klein tunneling ( $E < V_0$ ) and classical motion ( $E > V_0$ ).

Case 1: Klein tunneling ( $ss' = -1$ ). The transmission probability  $T$  can be given by Eq. (3), where

$$T = |t|^2 = \left[ \cos^2(q_x d) + \frac{(k_y^2 + k_F k_F')^2}{k_x^2 q_x^2} \sin^2(q_x d) \right]^{-1}. \quad (4)$$

Under the resonance conditions,  $q_x d = N\pi$ , ( $N=0, 1, \dots$ ), the transmission probability  $T$  is equal to 1. In addition, the barrier always remains perfectly transparent at the normal incidence  $\phi=0$ ,<sup>9</sup> which is so-called Klein paradox in quantum electrodynamics.<sup>21</sup> However, the transmission can be divided into evanescent and propagating modes, taking the influence of the parallel wave vector  $k_y$  into account. The electrons can tunnel through the potential barrier when  $\phi > \phi_c$ , where the critical angle for total reflection can be defined as

$$\phi_c = \sin^{-1} \left( \frac{V_0}{E} - 1 \right) \quad (5)$$

with the necessary condition  $E < V_0 < 2E$ . In this case, the transmission probability damped exponentially in the following form:

$$T \approx \frac{4k_x^2 q_x^2}{k_x^2 q_x^2 + (k_y^2 + k_F k_F')^2} e^{-2\kappa d}, \quad (6)$$

where  $\kappa = [k_y^2 - (E - V_0)^2 / \hbar^2 v_F^2]^{1/2}$  is the decay constant. As a matter of fact, the electrons can traverse through the potential barrier in propagating mode at any incidence angle, when the critical angle  $\phi_c$  is no longer valid for  $V_0 > 2E$ .<sup>9</sup> These results presented here can offer the complementary understanding of the evidence against Klein paradox in graphene.<sup>22,23</sup>

Case 2: Classical motion ( $ss' = 1$ ). The transmission probability can be rewritten as

$$T = \left[ \cos^2(q_x d) + \frac{(k_y^2 - k_F k_F')^2}{k_x^2 q_x^2} \sin^2(q_x d) \right]^{-1}. \quad (7)$$

Similarly, when the incidence angle  $\phi$  is less than the critical angle,

$$\phi'_c = \sin^{-1} \left( 1 - \frac{V_0}{E} \right) \quad (8)$$

the transmission probability  $T$  depends periodically on the width  $d$  of barrier. On the contrary, the electrons with the incidence angle of  $\phi > \phi'_c$  tunnel through the potential barrier with the transmission probability

$$T \approx \frac{4k_x^2 q_x^2}{k_x^2 q_x^2 + (k_y^2 - k_F k_F')^2} e^{-2\kappa d}. \quad (9)$$

Based on the properties in two cases of Klein tunneling and classical motion, the transmission as the function of incidence energy  $E$  has a gap, as shown in Fig. 2. Since  $q_x^2 = (E - V_0)^2 / \hbar^2 v_F^2 - k_y^2 < 0$ , the energy region of the transmission gap is given by  $V_0 - \hbar k_y v_F < E < V_0 + \hbar k_y v_F$ , which leads to the width of transmission gap as follows:

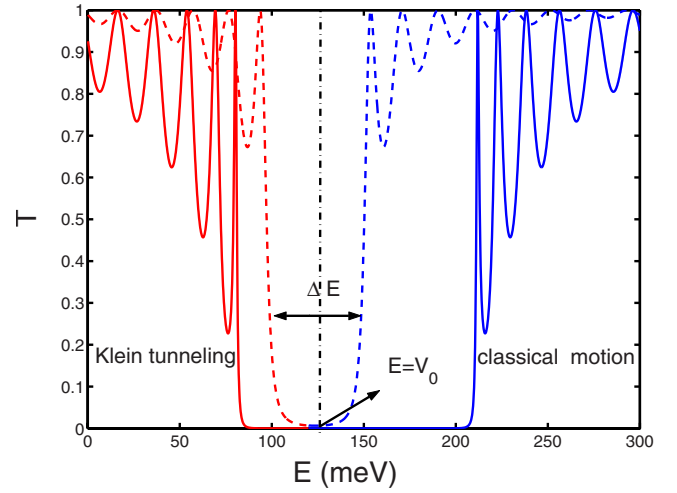


FIG. 2. (Color online) Transmission gap as the function of the incident energy  $E$ , where  $d=100$  nm and  $V_0=120$  meV. Solid and dashed curves correspond to  $\phi=25^\circ$  and  $10^\circ$ , respectively.

$$\Delta E = 2\hbar k_y v_F. \quad (10)$$

Obviously, the transmission gap with the center  $E=V_0$  becomes narrower with the decrease in the incidence angle and even vanishes at normal incidence. The transmission gap is due to the evanescent waves in two cases of Klein tunneling and classical motion so it has nothing to do with magnetic barriers in graphene<sup>16,17</sup> and is also quite different from that in graphene double barriers<sup>11</sup> or superlattices,<sup>12</sup> where the interference plays an important role in the transmission resonances and related transmission gap.

Figure 3(a) further indicates the dependence of the transmission gap on the width of potential barrier. It is indicated that the transmission gap will become deeper with the increase in the barrier width due to the decrease in the decay factor  $\exp(-2\kappa d)$  in Eqs. (6) and (9). The dependence of the transmission gap on the height of potential barrier and the incidence angle is also shown in Fig. 3(b). Interestingly, the center of the transmission gap can be controlled by changing the barrier height or strength (e.g., via adjusting a gate-voltage  $V_g$  in tunable graphene potential barrier).<sup>20</sup> That is to say, the incident energy can be selected by the tunable trans-

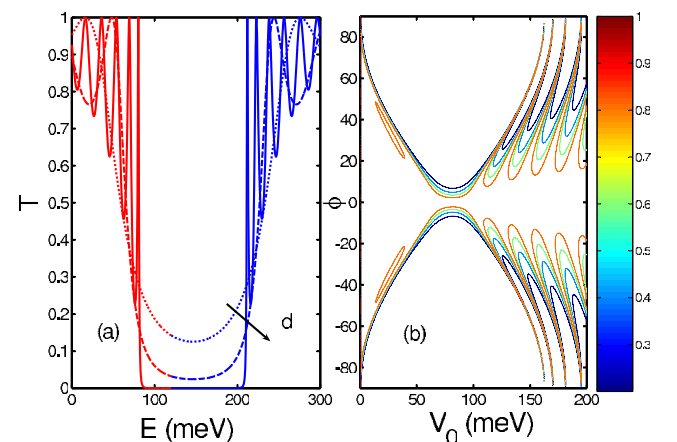


FIG. 3. (Color online) Dependence of transmission gap on the width and the height of potential barrier, where (a)  $V_0=120$  meV,  $\phi=25^\circ$ , solid, dashed, and dotted curves correspond to  $d=100, 30$ , and  $20$  nm. (b)  $E=80$  meV and  $d=100$  nm.

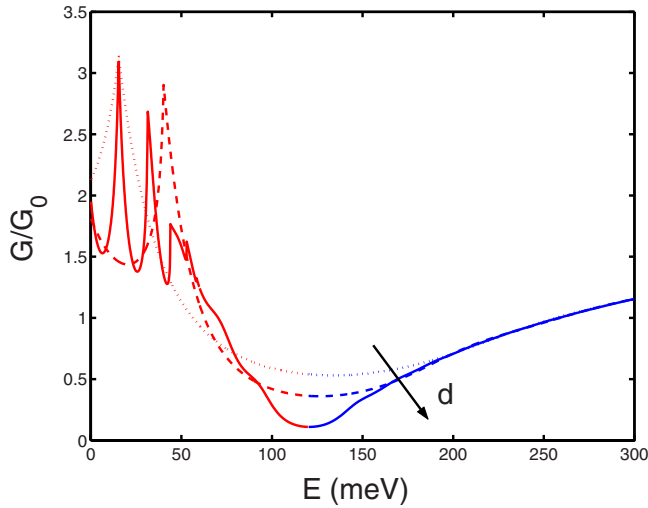


FIG. 4. (Color online) Conductance  $G$  as the function of incident energy, where the parameters are the same as in Fig. 3(a).

mission gap, which results in an alternative way to realize an electron wave energy filter. Moreover, the transmission gap discussed here is also related to the negative differential resistance.<sup>18</sup> In a word, the transmission gap in actual device structure can result in various graphene-based electronic devices.

In addition, the ballistic conductance under zero temperature is calculated by electron flow averaged over the half of the Fermi surface<sup>17,24</sup>

$$G = G_0 \int_{-\pi/2}^{\pi/2} T(E_F, E_F \sin \phi) \cos \phi d\phi, \quad (11)$$

with Fermi energy  $E_F$  and the units of conductance  $G_0 = (2e^2/\hbar)(\ell/\pi\hbar v_F)$ , where  $\ell$  is the length of the structure along the  $y$  direction. Figure 4 presents the conductance versus the variation in incidence energy  $E$ . It is shown that the visible kinks of the conductance due to transmission resonances are closely related to the quasibound states. More importantly, all conductance curves indicate a pronounced forbidden region, that is, the region of almost zero conductance corresponding to the transmission gap.

Finally, we have a brief look at the reflection. Figure 5 shows the reflection probability  $R = 1 - T$  as the function of Fermi wavelength  $\lambda$ . It is shown that the electron can be perfectly reflected by the graphene barrier. This pass band in reflection is analogous to Bragg reflection in optics, which is also found in magnetic barrier in graphene.<sup>25</sup> Actually, the Bragg-like reflection can also be applied to select electron wavelength or energy by the reflection window.

In summary, we investigate the transmission and reflection in 2D monolayer graphene barrier at the nonzero incidence angle. It is shown that the transmission gap as a function of the incident energy, which results from the evanescent waves in two cases of Klein tunneling and classical motion, can be controlled by the incidence angle, the height, and width of potential barrier. With the realization of the tunable potential barrier in graphene,<sup>20</sup> we hope these phenomena may lead to the potential applications in various graphene-based electronic devices.

This work was supported in part by the National Natural Science Foundation of China (Grant No. 60806041), the

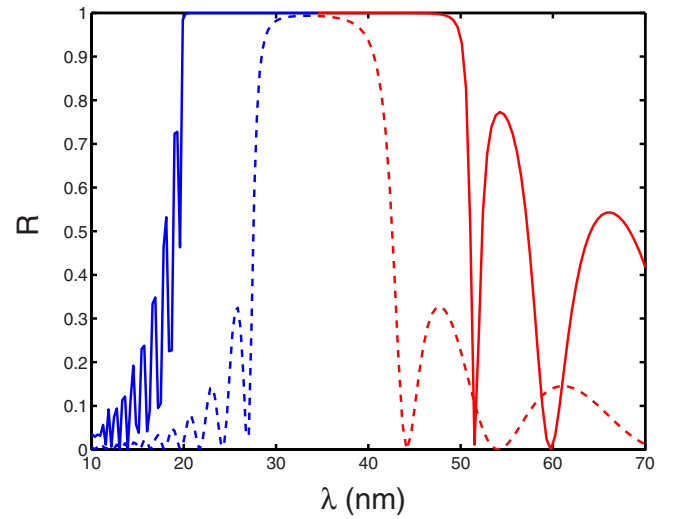


FIG. 5. (Color online) Reflection probability  $R$  as the function of  $\lambda$ , where the parameters are the same as in Fig. 2.

Shanghai Rising-Star Program (Grant No. 08QA14030), the Science and Technology Commission of Shanghai Municipal (Grant No. 08JC14097), the Shanghai Educational Development Foundation (Grant No. 2007CG52), and the Shanghai Leading Academic Discipline Program (Contract No. S30105). X.C. is also supported by Juan de la Cierva Programme of Spanish MICINN.

- <sup>1</sup>A. H. Castro Neto, F. Guinea, N. M. R. Peres, K. S. Novoselov, and A. K. Geim, *Rev. Mod. Phys.* **81**, 109 (2009).
- <sup>2</sup>C. W. Beenakker, *Rev. Mod. Phys.* **80**, 1337 (2008).
- <sup>3</sup>K. S. Novoselov, A. K. Geim, S. V. Morozov, D. Jiang, Y. Zhang, S. V. Dubonos, I. V. Grigorieva, and A. A. Firsov, *Science* **306**, 666 (2004).
- <sup>4</sup>K. S. Novoselov, *Mater. Today* **10**, 20 (2007).
- <sup>5</sup>M. I. Katsnelson and K. S. Novoselov, *Solid State Commun.* **143**, 3 (2007).
- <sup>6</sup>K. S. Novoselov, A. K. Geim, S. V. Morozov, D. Jiang, M. I. Katsnelson, I. V. Grigorieva, S. V. Dubonos, and A. A. Firsov, *Nature (London)* **438**, 197 (2005).
- <sup>7</sup>Y. Zhang, Y. W. Tan, H. L. Stormer, and P. Kim, *Nature (London)* **438**, 201 (2005).
- <sup>8</sup>V. P. Gusynin and S. G. Sharapov, *Phys. Rev. Lett.* **95**, 146801 (2005).
- <sup>9</sup>M. I. Katsnelson, K. S. Novoselov, and A. K. Geim, *Nat. Phys.* **2**, 620 (2006).
- <sup>10</sup>J. M. Pereira, V. Mlinar, F. M. Peeters, and P. Vasilopoulos, *Phys. Rev. B* **74**, 045424 (2006).
- <sup>11</sup>J. M. Pereira, Jr., P. Vasilopoulos, and F. M. Peeters, *Appl. Phys. Lett.* **90**, 132122 (2007).
- <sup>12</sup>C.-X. Bai and X.-D. Zhang, *Phys. Rev. B* **76**, 075430 (2007).
- <sup>13</sup>A. DeMartino, L. Dell'Anna, and R. Egger, *Phys. Rev. Lett.* **98**, 066802 (2007); *Solid State Commun.* **144**, 547 (2007).
- <sup>14</sup>M. Ramezani Masir, P. Vasilopoulos, A. Matulis, and F. M. Peeters, *Phys. Rev. B* **77**, 235443 (2008).
- <sup>15</sup>F. Zhai and K. Chang, *Phys. Rev. B* **77**, 113409 (2008).
- <sup>16</sup>M. Ramezani Masir, P. Vasilopoulos, and F. M. Peeters, *Appl. Phys. Lett.* **93**, 242103 (2008).
- <sup>17</sup>M. Ramezani Masir, P. Vasilopoulos, and F. M. Peeters, *Phys. Rev. B* **79**, 035409 (2009).
- <sup>18</sup>D. Dragoman and M. Dragoman, *Appl. Phys. Lett.* **90**, 143111 (2007).
- <sup>19</sup>S. Garg, R. K. Sinha, and K. L. Deori, *Semicond. Sci. Technol.* **18**, 292 (2003).
- <sup>20</sup>B. Huard, J. A. Sulpizio, N. Stander, K. Todd, B. Yang, and D. Goldhaber-Gordon, *Phys. Rev. Lett.* **98**, 236803 (2007).
- <sup>21</sup>N. Dombey and A. Calogeracos, *Phys. Rep.* **315**, 41 (1999).
- <sup>22</sup>S. P. Bowen, arXiv:0807.3592v1.
- <sup>23</sup>D. Dragoman, *Phys. Scr.* **79**, 015003 (2009).
- <sup>24</sup>A. Matulis, F. M. Peeters, and P. Vasilopoulos, *Phys. Rev. Lett.* **72**, 1518 (1994).
- <sup>25</sup>S. Ghosh and M. Sharma, arXiv:0806.2951v4.